Supporting Information

D-fructose Molecule Template Route to Ultrathin $ZnSnO_3$ Nanowire Architectures and Their Application as Efficient Photocatalyst

Caihong Fang, Baoyou Geng*, Jun Liu, and Fangming Zhan

College of Chemistry and Materials Science, Anhui Key Laboratory of Functional Molecular Solids, Anhui Normal University，Wuhu, 241000, P. R. China.

E-mail: bygeng@mail.ahnu.edu.cn

1. Experimental section

The $ZnSnO_3$ architectures were synthesized by a molecule route. The zinc acetate ($ZnAc_2·2H_2O$, analytical grade) and tin tetrachloride ($SnCl_4·5H_2O$, analytical grade) were used as starting materials without further purification. D-fructose was used as molecular template. The starting materials were dissolved into distilled water to form two individual transparent solutions. The preparation of $ZnSnO_3$ is based on the following reaction:

$$ZnAc_2 + SnCl_4 + 6NaOH = ZnSnO_3 + 4NaCl + 2NaAc + 3H_2O$$

In a typical synthesis, 0.225 g D-fructose was added into 5 mL of 0.5 M $ZnAc_2$ solution in water (at room temperature) under vigorous agitation. And then 5 mL of 0.5 M $SnCl_4$ solution and 10 ml sodium hydroxide (NaOH, 3.0 M) solution were added into the mixture to form a uniform suspension. Then the suspension was transferred into a 30 mL Teflon-lined stainless-steel autoclave. The autoclave was maintained at a temperature 180 °C for 12 h without stirring and shaking. In the end, the white products were collected by centrifugation and washed repeatedly with ethanol before characterization and study. The homemade $ZnSnO_3$ powders were synthesized through the similar process as above without adding D-fructose in the reaction system.

X-ray powder diffraction (XRD) was carried out on an XRD-6000 (Japan) X-ray diffractometer with Cu-Kα radiation (λ=1.54060 Å) at a scanning rate of 0.05 $°\cdot s^{-1}$. Scanning electron microscopy (SEM) micrographs were taken using a Hitachi S-4800 Scanning electron microscope. Transmission electron microscopy (TEM) micrographs and High-resolution transmission electron microscopy (HRTEM) was performed using JEM 2010 F microscopes operated at optimum defocus with accelerating voltages of 200 kV and energy-dispersive X-ray spectroscope (EDS) attached to the TEM. Specific surface areas and pore size distribution were computed from the results of N_2 physisorption at 77 K (model: BECKMAN SA3100 COULTER) using the BET (Brunauer-Emmet-Teller).

The photocatalytic activity experiments on the obtained $ZnSnO_3$ for the decomposition of Rhodamine B in air were performed at ambient temperature. A cylindrical Pyrex flask (capacity ca. 100 mL) was used as the photoreactor vessels. $ZnSnO_3$ product as catalyst (3 mg) was added in the aqueous Rhodamine B solution (2.0×10^{-5} M, 50 mL) and was magnetically stirred in the dark for 10 min and then exposed to ultraviolet (UV) (250 W, λ=365 nm). As a comparison, the photocatalytic activities of $ZnSnO_3$ powders (homemade) and commercial TiO_2

powders (Degussa P25, Degussa Co. the surface area is ca. 45 m^2g^{-1}) were also tested at the same experimental conditions. UV-vis absorption spectra were recorded at different intervals to monitor the reaction using U-4100 UV/vis spectrophotometer. Diffuse reflectance UV-vis absorption spectra were measured with a Shimadzu Model UV-2450 UV-vis spectrophotometer in the wavelength range of 200-800 nm. And the MgO served as a reference sample.

2. XRD pattern of the as-prepared $ZnSnO_3$ architectures.

Fig. S1 shows the XRD pattern of the as-prepared $ZnSnO_3$ architectures. The corresponding XRD diffraction peaks of the products can be all indexed to a pure $ZnSnO_3$ (JCPDS: 11-0274). No peaks from other phases can be detected, thus indicating that the products are pure high crystalline.

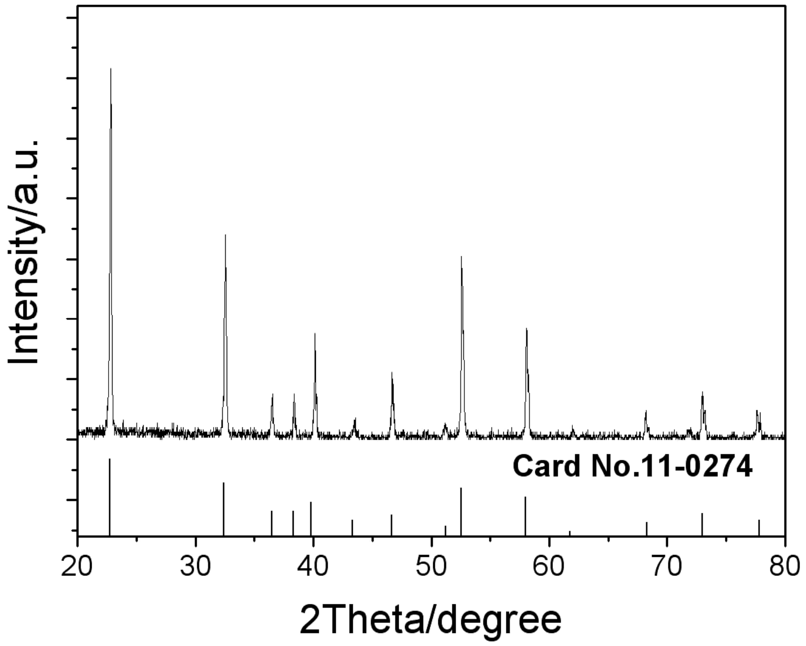

Fig. S1 The corresponding XRD pattern of the as-prepared $ZnSnO_3$ architectures.

3. BET measurement of the obtained $ZnSnO_3$ architectures.

Full nitrogen sorption isotherms were measured to gain information about specific surface area of the obtained $ZnSnO_3$ architectures, as shown in Figure S2. The adsorption curve is of a reverse 'S'-shape, which is a normal physical adsorption isotherm. The specific surface area was thus evaluated to be 191.2 m^2 g^{-1} from data points in this pressure range by the BET equation.[1] Obviously, the ultra-thin $ZnSnO_3$ architectures with high specific surface area will be stabile against aggregation, and may exhibit potential application in catalysis and sensing.

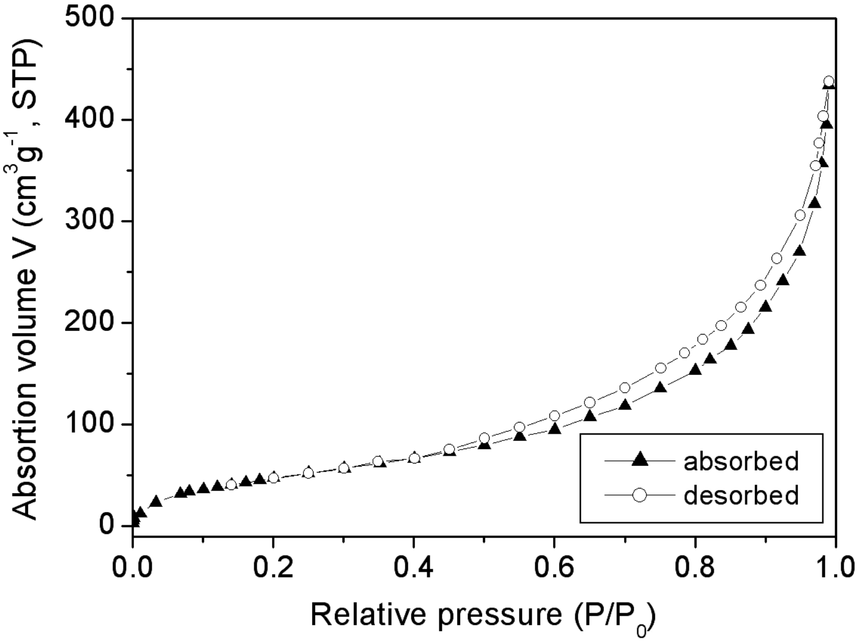

Fig. S2 Full nitrogen sorption isotherms of the as-prepared $ZnSnO_3$ architectures.

4. SEM image and XRD pattern of the homemade $ZnSnO_3$ powders.

Fig. S3 shows the SEM image and XRD pattern of the homemade $ZnSnO_3$ powders. The SEM image shows that the obtained products are powder-like morphology. The corresponding XRD pattern can also be indexed to a pure $ZnSnO_3$ (JCPDS: 11-0274).

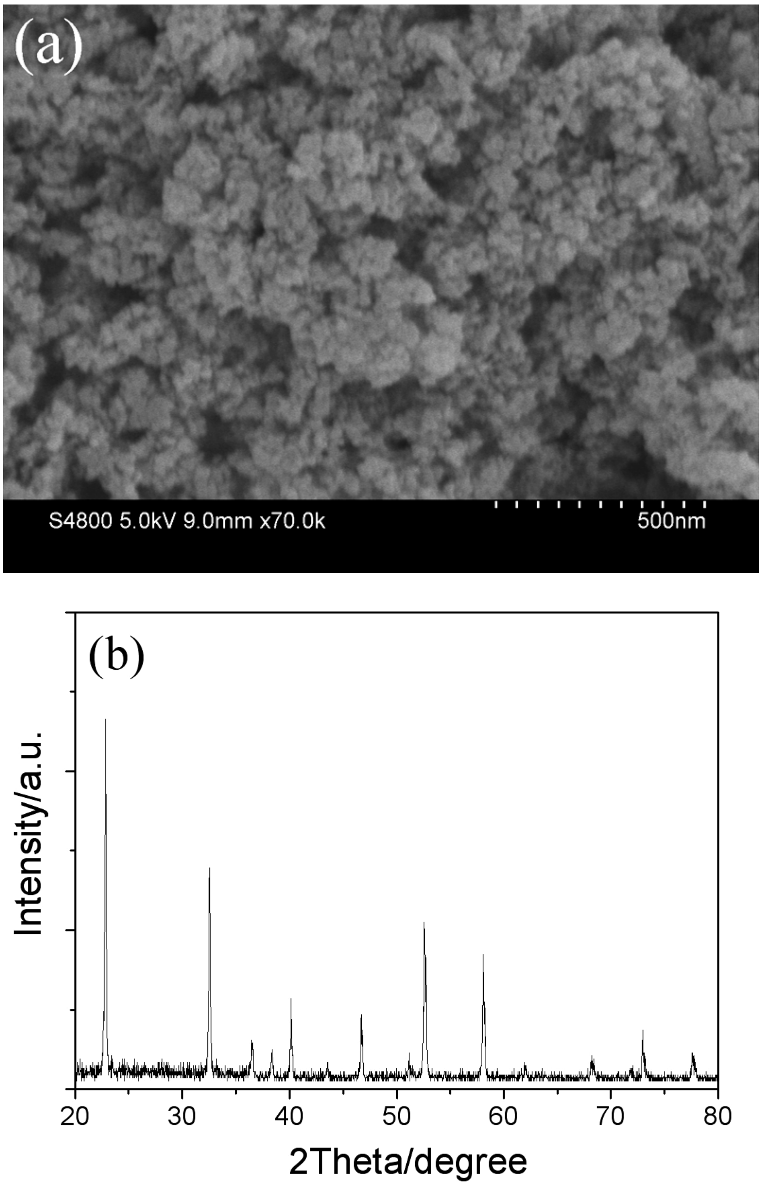

Fig. S3 SEM image (a) and XRD pattern (b) of the homemade $ZnSnO_3$ powders.

5. The durability of photocatalytic activity.

The durability of photocatalytic activity was performed by reusing of the catalysts in RB under UV light irradiation respectively using the $ZnSnO_3$ architectures and

P25 (20 min irradiation for each cycle). The photodegradation results were shown in Fig. S2 which shows that the P25 exhibits good durability and the decolorization percentage decreased from 32 % to 29 % after four cycles. Comparatively, it was found that the $ZnSnO_3$ architectures exhibit better durability than that of the P25. The results of decolorization percentage demonstrate that there is no significant change in the activity even after the fourth cycle. The decolorization percentage decreased from 100 % to only 98.5 % after four cycles. The above results show that the obtained $ZnSnO_3$ architectures exhibit much higher photocatalytic performance as well excellent durability than those of the P25.

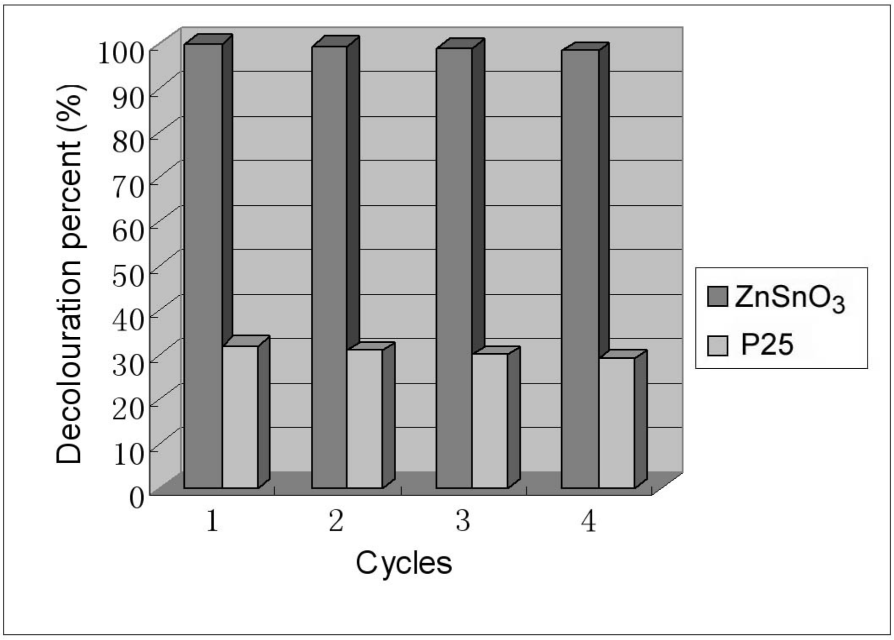

Fig. S4 The comparison of photodegradation performance within four cycles for the architectured $ZnSnO_3$ and titania. 1 the original test. 2 the first recycle. 3 the second recycle. 4 the third recycle.

6. The diffuse reflectance UV-vis spectra of the $ZnSnO_3$ architectures and powders.

Fig. S5 reveals that both the $ZnSnO_3$ architectures and $ZnSnO_3$ powders have apparent absorption band edges, which demonstrate that they exhibit semiconducting property. Compared with the $ZnSnO_3$ powders, the absorption band edge of the $ZnSnO_3$ architectures shows a clear blue-shift, which should be attributed to the quantum size effects.

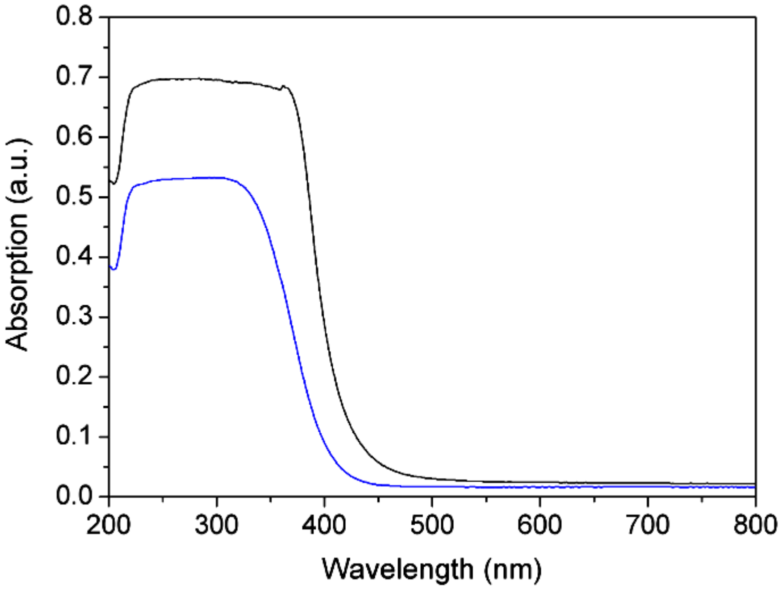

Fig. S5 Diffuse reflectance spectra of the $ZnSnO_3$ architectures (blue line) and powders (black line).

Reference

[1] S. Brunauer, P. H. Emmett, E. Teller, *J. Am. Chem. Soc.* 1938, **60**, *309*.